TALUS, SOLIFLUCTION AND RAISED MARINE DEPOSITS AT CAPE RICKETTS, S.W. DEVON ISLAND, N.W.T.

- a study of the size and shape characteristics of surface mantle materials in an Arctic environment

R. L. Cox

4c6 Research Paper submitted as part of the degree requirements in Geography at McMaster University, Hamilton.

April 20, 1969

ACKNOWLEDGMENTS

The field work was carried out as part of a research project by McMaster University under the direction of Dr. S.B. McCann whose guidance and encouragement were much appreciated. A further note of appreciation is expressed to Mr. E. H. Owens and Mr. D. R. Ingram for technical and field assistance, as well as to the Arctic Institute of North America and the Continental Polar Shelf Project for logistic support.

CONTENTS

LIST OF MAPS

LIST OF TABLES

LIST OF PHOTOGRAPHS

G. 1

MAP OF TOPIC AREA LOCATION

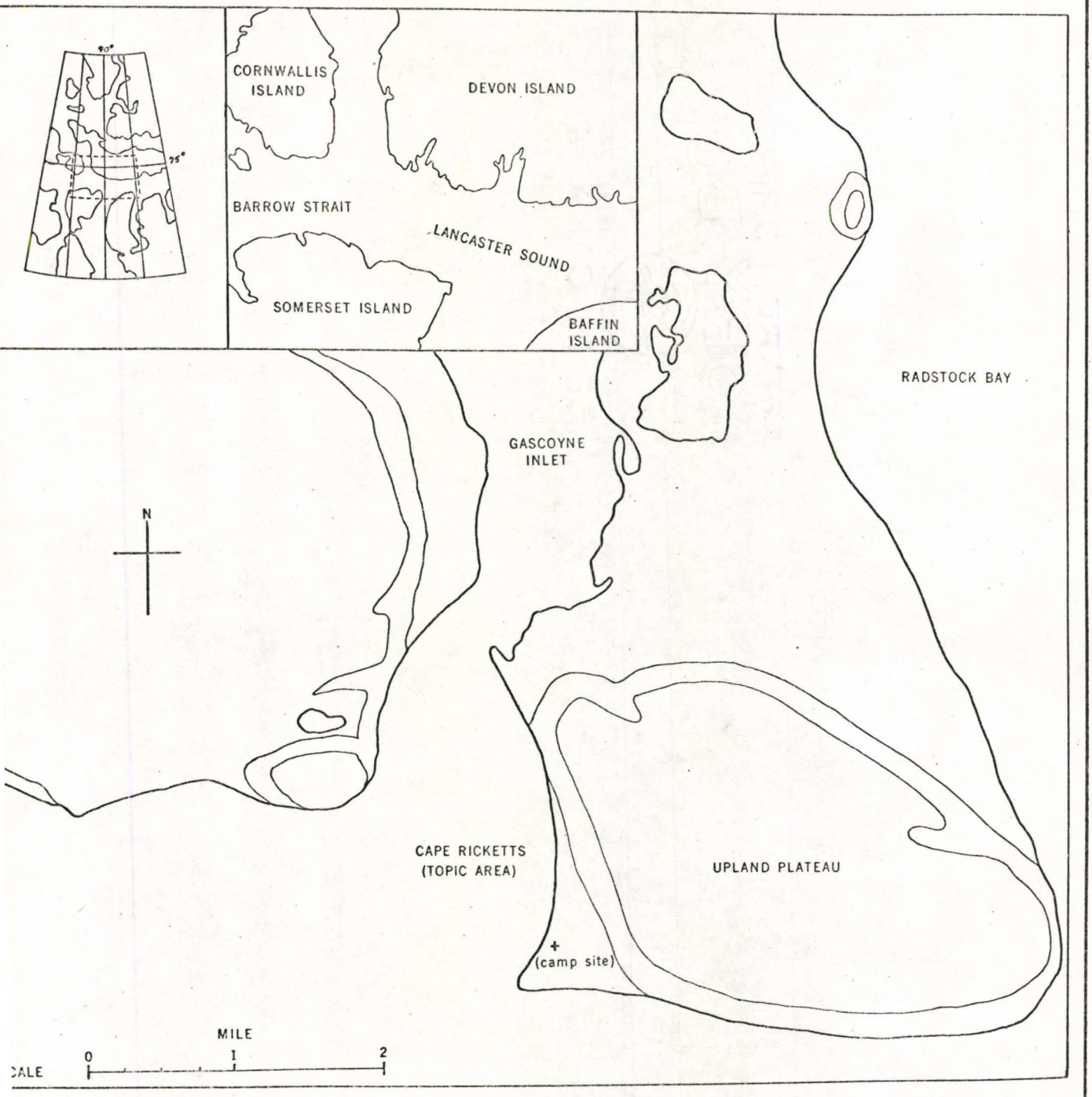

CHAPTER I

Introduction

> "There is no doubt that process and the related landforms, in Arctic areas, produce a distinct morphogenetic system, but whether this progresses in definable stages is open to question".
>
> (J.B. Bird 1967, p. 423)

Within the periglacial environment of the Canadian Arctic Archipelago three main physiographic units exist in the landscape - plateau areas, which make up much of the interior, cliffs and talus slopes, which constitute the seaward margins of the plateau areas, sometimes forming the actual coastline but frequently being separated from the sea by the third landscape unit, the series of recently emerged strandlines (photo 1). Solifluction, the mass movement of water soaked debris, is one of the main agents of denudation producing a characteristic assenblage of surface forms. The most marked area of solifluction occurs at the base of the talus slopes where solifluction material is superimposed on the upper slopes of raised marine deposits.

This paper presents a study of the sequential modification of the surface mantle of the coastal foreland at Cape Ricketts on S.W. Devon Island (latitude 75°N., longitude 90°W.) in what is considered to represent a type situation often repeated within the overall landscape of Devon and Cornwallis Islands. Thus it is hoped that the observations and conclusions relating to this particular area will have a more general application.

Composed of horizontally bedded Paleozoic sandstones, limestones, dolomites and shales S.W. Devon Island is essentially devoid of structural relief. Isostatic emergence subsequent to glacial submergence has engendered relief up to 1100 feet, concentrated along the seaward margins of the upland plateau as a series of alternating cliffs and fiord-like inlets.

The Cape Ricketts depositional foreland, located on the S.W. periphery of an isolated upland plateau area, constitutes the eastern shore of the entrance to Gascoyne Inlet (Fig. 1). Three major morphological zones can be recognised below the plateau at Cape Ricketts:- a series of strandlines of raised marine material, extending inland from the modern beach but becoming obscured upslope by a second zone of overriding solifluction material, which ends abruptly further inland at the base of the higher talus slopes, making up the third zone. The zone of solifluction exhibits two different types of movement, exhibiting different surface expression, thus it is convenient to consider it as two separate zones, termed the upper and lower solifluction zones. Since it is also feasible to give the modern beach the status of a definable morphological unit, to separate it from the raised beach zone, then the original three broad zones are increased to five (fig. 2).

Sequential development of these five proposed zones is modified, in the topic area, by three factors. The first, and most significant being a large depositional terrace providing a disproportionate amount of finer material which is moved downslope by the second modifying agent, surface stream action and rill wash, to distend the solifluction zones downslope, and thirdly a boulder field to the north which inhibits this extension.

Specifically, the purpose of this paper is to compare inter-zonal and intra-zonal, downslope and alongslope, variations of certain commonly used sediment size and shape parameters derived from analysis of the mantle material. In this manner it is hoped to establish the validity of the suggested zones and to give some quantitative expression to the differences between zones in terms of the character of the superficial material (photo 2).

Numerous studies have been undertaken which attempt to interpret and distinguish between different depositional environments by considering various measures of the size distribution of the sediments concerned. These have largely been carried out on coastal, marine and to a lesser extent, fluvial deposits (e.g. Folk and Ward, 1957, and Mason and Folk, 1958). Investigations into the shape of sedimentary particles has also permitted a distinction in quantitative terms between various environments of deposition (e.g. King and Buckley, 1968). By considering both the size and shape characteristics of the mantle material at Cape Ricketts within the areal context of the proposed system of five morphological zones it was hoped that some useful comments could be made concerning the query raised in the quotation at the beginning of this introduction.

ZONE MAP OF TOPIC AREA

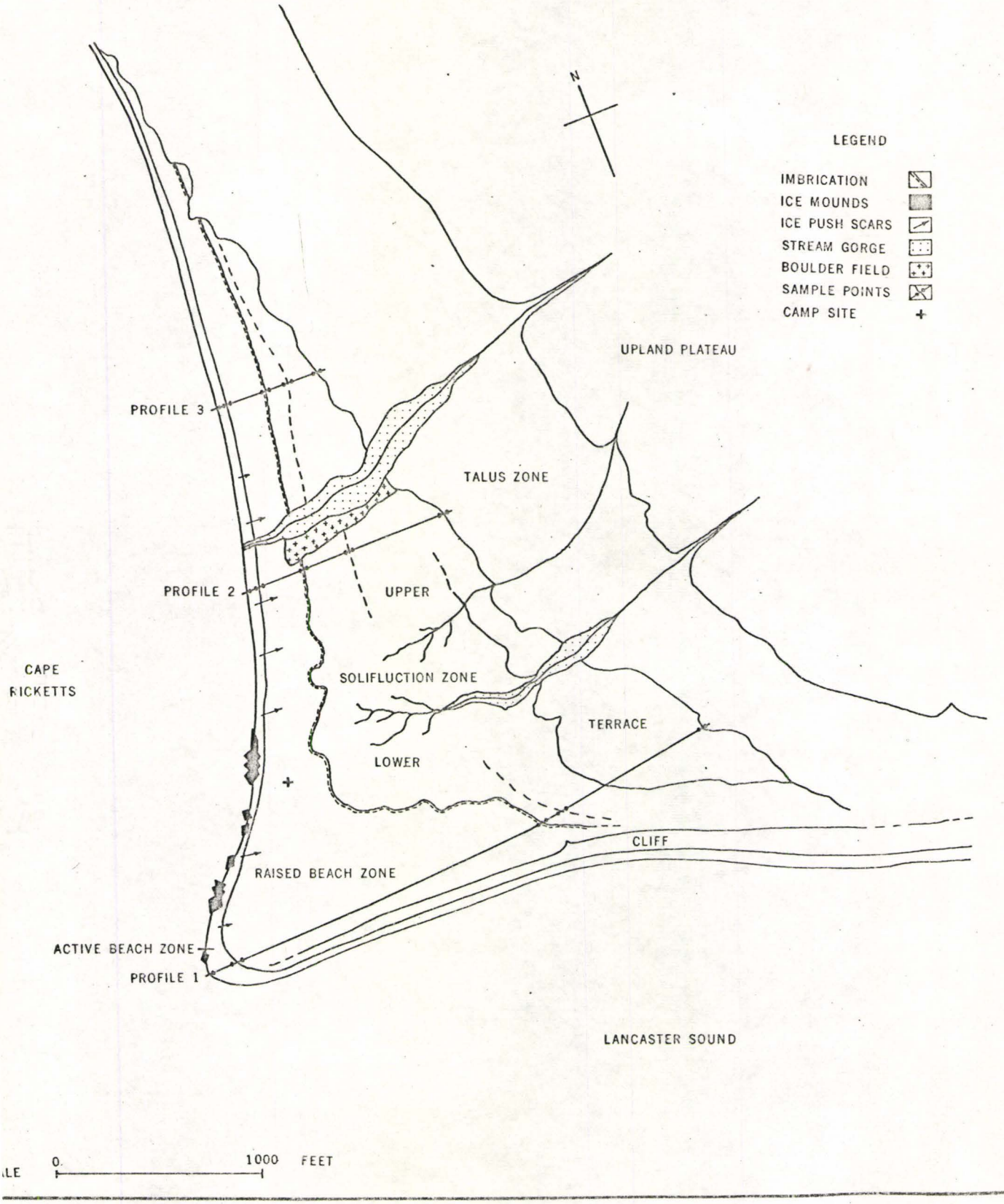

CHAPTER II

Field Procedure and Methods of Analysis

In order to collect meaningful data a sampling grid was established by surveying three profiles, each running due east upslope and perpendicular to the proposed zones. These survey lines were tied to mean sea level by means of a later tachiometric survey. Two sample points were marked in each proposed zone along each profile line and an appropriate sample number painted on a rock slab placed at the sample point. Located approximately ten feet from the upper and lower limits of each zone the sample points were chosen to best illustrate changes expected within the zones as well as between the zones. This procedure was carried out in all zones except the talus where only the lower limit of the slope was sampled, since the surface material appeared homogeneous in nature and upper limit sampling was both arbitrary and dangerous. Twenty-seven sample points in all were thus established.

Samples were collected from the upper 1" of the surface material at each sample point, each sample containing approximately 600 grams. If the samples were wet, they were dried in a hand made kiln before being ground with a pestle and mortar to break up the peds. The samples were then dry sieved by hand using a British Standard sieve set, dividing the sample materials into phi groups. Inman (1952) introduced the phi scale by converting the Wentworth grade scale, based on diameter in millimeters, according to the formulae; $\phi = \log_2 d$,

where d is the diameter in millimeters. A phi range was chosen from +1.0 phi to -6.0 phi inclusive at one phi intervals. This range proved sufficient for the material sampled since all material smaller than 0.0 phi was classed as +1.0 and termed fines. The material of each phi size within each sample was then weighed and recorded in the field.

Later analysis was carried out utilising the sedanl fortran computer program, produced by the Woods Hole Oceanographic Institute (Schlee and Webster, 1965) for sediment size analysis which was modified to accept the above data by Mr. D. R. Ingram. The sedanl program computed percentages and cumulative percentages of phi sizes by weight, the mode(s) and the median as well as the first four moment measures of the phi size distributions. A graph of the distributions of material weight in grams was plotted against phi size to complete the computations for each sample.

Samples of the fines collected from profiles 1 and 2 were brought back to the laboratory for further analysis. Each sample was oven dried, then separated by mechanical sieving using a British Standard sieve set. The range of from 0.0 phi to +5.0, at one phi intervals, was chosen. Each phi size was then recorded as to weight.

These samples, in composite form, were also analyzed for their carbonate contents. The method follows that outlined for the Collins Calcimeter and all results were expressed as percentage carbonate weights and recorded for each sample.

At each field sample point a representative twenty stones were collected and measured for shape characteristics, a maximum of

120 mm and a minimum of 4 mm were arbitrarily chosen as the limits of measurable material for reasons of ease and accuracy of measurement. Length, width and thickness (denoted as A, B and C respectively) were measured using a transparent millimeter rule. A measure of angularity was obtained by fitting the radius of least curvature of each stone to a chart of concentric circles of specified metric diameter, (Cailleux & Tricart, 1963) and recorded as a value of R.

These data were processed by a Boulder Roundness program written by J. C. Goldi of the former Canadian Geographical Branch. The following equations were computed in this program to produce the desired shape parameters;

roundness factor $\frac{2R}{A} \times 1000$ (Cailleux)

flatness factor $\frac{A + B}{2C} \times 100$ (Cailleux)

sphericity factor $\sqrt[3]{\frac{B.C}{A^2}}$ (Krumbein)

For each sample the four moment measures of roundness, flatness, sphericity and length were computed and printed. This was supplemented by frequency and cumulative curve photo at convenient intervals for each of the four factors.

To the measurements of size and shape, slope in degrees, percentage of fines by weight and percentage of free carbonates by weight were recorded for each sample to provide 23 indicators of surface material characteristics. Listed in Table 1 are those variables used in the analysis.

Further justification of the above methods may be made on a number of grounds. The topic area was conducive to the sampling

TABLE I

DATA RESULTS FROM COMPUTATION AND LABORATORY ANALYSIS

Field Sample	Sample Number	Zone	Mean Roundness	Mean Flatness	Mean Sphericity	Mean (mm) Length	Slope in Degrees
1.1	01	A	235.0	367.5	0.565	34.5	0
1.3	04	A	222.5	320.0	0.595	32.5	2
1.3A	05	R	72.5	512.5	0.525	36.0	7
1.4	09	R	227.5	242.5	0.625	20.5	2
1.5	10	LS	120.0	317.5	0.585	31.5	5
1.6	11	LS	165.0	420.0	0.560	32.5	5
1.7	12	US	130.0	332.5	0.560	37.0	12
1.8	13	US	82.5	465.0	0.515	47.0	8
1.9	14	T	27.5	317.0	0.590	42.0	25
2.1	01	A	225.0	325.0	0.600	42.5	5
2.2	02	A	210.0	530.0	0.510	56.5	5
2.3	03	R	155.0	450.0	0.515	33.5	5
2.4	04	R	145.0	495.0	0.505	40.0	5
2.5	06	LS	177.0	305.0	0.655	24.5	5
2.6	07	LS	185.0	317.5	0.590	24.5	5
2.7	08	US	120.0	462.5	0.535	30.0	7
2.8	09	US	167.5	355.0	0.585	32.0	14
2.8	10	T	27.5	312.5	0.610	37.0	30
3.1	01	A	137.5	392.5	0.555	48.0	7
3.2	02	A	152.5	435.0	0.545	45.5	7
3.3	03	R	140.0	655.0	0.460	49.5	6
3.4	04	R	117.5	675.0	0.445	41.0	6
3.5	05	LS	217.5	450.0	0.510	31.5	5
3.6	06	LS	57.5	347.5	0.605	30.5	5
3.7	07	US	75.0	437.5	0.575	29.0	8
3.8	08	US	87.5	295.0	0.610	37.5	8
3.9	09	T	30.0	245.0	0.640	48.0	32

A - active beach

R - raised beach

LS - lower solifluction

US - upper solifluction

T - talus

TABLE 1 (continued)

Field Sample	Sample Number	Zone	Mean Size in Phi Units	Mean Standard Deviation	Mean Skewness	Mean Kurtosis	% Fines by Weight	% Free Carbonates by Weight
1.1	01	A	-3.30	1.13	0.37	1.57	t	N
1.3	04	A	-4.10	0.97	0.00	0.25	t	N
1.3A	05	R	-3.82	1.59	0.79	4.42	3.9	30.8
1.4	09	R	-1.75	2.38	0.24	0.05	21.5	36.0
1.5	10	LS	-2.92	2.20	0.91	1.38	12.2	26.0
1.6	11	LS	-3.09	1.63	1.08	6.08	5.2	23.7
1.7	12	US	-4.60	1.30	1.84	---	3.3	61.1
1.8	13	US	-4.79	1.76	1.53	---	4.7	25.9
1.9	14	T	-5.40	0.50	0.46	2.28	t	N
2.1	01	A	-4.26	1.03	0.07	0.18	t	N
2.2	02	A	-5.24	0.84	0.52	1.28	t	N
2.3	03	R	-4.83	0.85	0.25	-0.45	t	N
2.4	04	R	-4.62	0.97	0.70	4.75	1.8	N
2.5	06	LS	-1.90	2.62	0.51	0.01	40.1	23.0
2.6	07	LS	-1.52	2.48	0.42	-0.04	50.5	23.0
2.7	08	US	-2.35	2.43	0.61	1.00	50.1	24.2
2.8	09	US	-4.06	1.44	0.65	1.46	6.2	N
2.8	10	T	-5.45	0.80	0.50	7.21	t	N
3.1	01	A	-4.93	0.90	0.43	0.43	t	N
3.2	02	A	-4.35	1.12	0.06	-0.71	t	N
3.3	03	R	-4.96	0.76	0.50	3.29	3.2	N
3.4	04	R	-4.81	0.85	0.50	2.96	8.6	N
3.5	05	LS	-3.55	1.74	0.37	-0.25	25.8	N
3.6	06	LS	-3.60	2.00	0.39	-0.68	26.2	N
3.7	07	US	-2.91	1.66	0.25	-0.74	25.6	N
3.8	08	US	-4.61	1.65	0.91	2.45	7.6	N
3.9	09	T	-5.45	0.65	0.38	0.74	t	N

t - trace

N - not sampled

technique due to the stunted nature and sparse distribution of vegetation, the relatively recent age of the landform (King & Buckley, 1968) and the ease with which the different slope segments could be visually distinguished, sampling methods, for the most part, allowed data collection in the field simply, inexpensively and relatively quickly. Most significantly the type of data measurements facilitated comparison, in terms of relevance and accuracy, with a substantial number of size and shape investigations carried out in the past.

CHAPTER III

Quantitative Analysis

Prior to a detailed discussion of the five proposed zones their quantitative existence in terms of surface size and shape characteristics will be established. To accomplish this, a method for determining the degree of randomness of the data values used was employed. This method, produced by Cadigan (1952), uses the highly sensitive Chi-square index. The differences between the observed and the expected values yields a computed Chi-square value producing a probability range of randomness. For the purposes of the test a significance level of 5 percent (probability of randomness, Pr = 0.05) or smaller was considered evidence of non-randomness.

Table 2 is a grid of roundness values calculated according to Cailleux' formula $\frac{2R}{A} \times 1000$ and represents the distribution of these values across the topic area. Since the relative positions of the sample points have been maintained the distortion of the dimensions of the area to those of the grid pattern does not affect the test. A further assumption has been made. Two samples were taken from each zone along each profile, except in the talus zone where only one sample was collected. The angularity or roundness of the talus material is assumed to be the same if not less on the upper slopes of the talus zone since it is nearer the origin of the rock fragments. The roundness values for sample 9 were, therefore, considered as representative

of 2 samples and a tenth sample point was added to each profile, thus reducing bias in the test.

A median was calculated for the roundness values and each grid square was marked as above the median (black triangle) or below the median (white triangle). The grid was then divided into 5 groups, each consisting of 6 grid squares, numbered I, II, III, IV, and V, (Table 2).

A hypothesis that the roundness values were randomly distributed over the area, was stated. Therefore, of the 30 roundness values, 15 were expected to be high values and 15 low values. Similarly 15/30th or 50% of the 6 squares in each group (3) were expected to be high and 3 low. The Chi-square index was computed for each group according to the following formula:

$$x^2 = \frac{(O_1 - E_1)^2}{E_1} + \frac{(O_2 - E_2)^2}{E_2} + \ldots \frac{(On - En)^2}{n}$$

where E = expected values

O = observed values

The probability was then obtained from the computed Chi-square index, a known degree of freedom (n - 1) and table of Chi-square values (attached) computations are given below for group I.

$$\text{unadjusted } x^2 = \frac{(0 - 3)^2}{3} + \frac{(6 - 3)^2}{3}$$

$$= 3.000 + 3.000$$

$$= 6.000$$

To adjust for theoretical bias because there are only 2 subsamples

TABLE 2

ROUNDNESS VALUES USED IN THE CADIGAN RANDOMNESS TEST

SAMPLE NUMBER	Profile Number 3	2	1	GROUP NUMBER
(10)	30.0	27.5	27.5	I
9	30.0	27.5	27.5	
8	87.5	167.5	82.5	II
7	75.0	120.0	130.0	
6	57.5	185.0	165.0	III
5	217.5	177.0	120.0	
4	117.5	145.0	277.5	IV
3	140.0	155.0	72.5	
2	152.5	210.0	107.5	V
1	137.5	225.0	235.0	

27.5	
27.5	
27.5	Section A
27.5	9
30.0	
30.0	
57.5	
72.5	
75.0	
82.5	
87.5	
117.5	
120.0	Section B
120.0	(11)
130.0	
	Median
137.5	
140.0	
145.0	
152.5	
155.0	
165.0	
167.5	
167.5	Section C
177.0	(10)
185.0	
210.0	
217.0	
225.0	
227.0	
235.0	

Median Roundness Value = 132.8

above median value 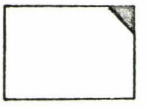

below median value 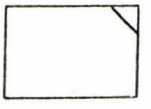

and less than 200 values, 0.5 is subtracted from each absolute quantity (O - E), therefore:

$$\text{adjusted } x^2 = \frac{(2.5)^3}{3} + \frac{(2.5)^2}{3}$$

$$= 2.080 + 2.080$$

$$= 4.160$$

As seen from the Table 3 of the distribution of Chi-square values, the value of 4.160, with (n - 1) or 1 degree of freedom, the probability of randomness (Pr) is found to lie between 0.05 and 0.02. Thus the hypothesis of random distribution is not supported by the proportions of high and low values in group I.

The complete test results are shown in Table 3 where the probability of randomness of each of the groups and for the whole area are listed. The Pr of less than 0.01 indicates the 5 group Chi-square indices have a very low probability of occurring in a situation of randomly distributed values. Therefore the initial hypothesis of random distribution could be rejected well within the 0.05 level of significance.

The same test was carried out using sphericity values obtained from Krumbein formula $\sqrt[3]{\frac{B.C}{A^2}}$, and using phi size values from Inman's conversion of the Wentworth size scale. In both cases the hypothesis, that the values were randomly distributed over the area, was rejected on the basis of a 0.05 level of significance.

Roundness values were next divided into 3 sections. Section A included values from 0 to 80.0, section B from 81.0 to 160.0 and section C from 161 to 240.0 (refer to Table 2). The nullhypothesis, that the

TABLE 3

SUMMARY OF CHI-SQUARE RESULTS FOR ROUNDNESS (GROUP) VALUES

Group	Number of Values	Observed High	Observed Low	Expected High	Expected Low	Computed Chi-Square (Unadjusted)	Computed Chi-Square (Adjusted)	Degrees of Freedom	Probability of Randomness (Pr)
I	6	0	6	3	3	6.000	4.160	1	0.05 - 0.02
II	6	1	5	3	3	2.667	1.500	1	0.50 - 0.20
III	6	4	2	3	3	0.667	0.167	1	0.80 - 0.50
IV	6	4	2	3	3	0.667	0.167	1	0.08 - 0.50
V	6	6	0	3	3	6.000	4.160	1	0.05 - 0.02
Sum of Chi-Squares						16.001		5	0.01
Total for Area	30	15	15	15	15				

DISTRIBUTION OF CHI-SQUARE (x^2)

814 *R. A. CAJDIGAN*

TABLE 1.—*Distribution of Chi-square* (X^2)[1]

Degree of freedom	Probability										
	0.99	0.98	0.95	0.90	0.80	0.50	0.20	0.10	0.05	0.02	0.01
1	0.00016	0.00063	0.00393	0.0158	0.0642	0.455	1.642	2.706	3.841	5.412	6.635
2	.0201	.0404	.103	.211	.446	1.386	3.219	4.605	5.991	7.824	9.210
3	.115	.185	.352	.584	1.005	2.366	4.642	6.251	7.815	9.837	11.345
4	.297	.429	.711	1.064	1.649	3.357	5.989	7.779	9.488	11.668	13.277
5	.554	.752	1.145	1.610	2.343	4.351	7.289	9.236	11.070	13.388	15.086
6	.872	1.134	1.635	2.204	3.070	5.348	8.558	10.645	12.592	15.033	16.812
7	1.239	1.564	2.167	2.833	3.822	6.346	9.803	12.017	14.067	16.622	18.475
8	1.646	2.032	2.733	3.490	4.594	7.344	11.030	13.362	15.507	18.168	20.090
9	2.088	2.532	3.325	4.168	5.380	8.343	12.242	14.684	16.919	19.679	21.666
10	2.558	3.059	3.940	4.865	6.179	9.342	13.442	15.987	18.307	21.161	23.209
11	3.053	3.609	4.575	5.578	6.989	10.341	14.631	17.275	19.675	22.618	24.725
12	3.571	4.178	5.226	6.304	7.807	11.340	15.812	18.549	21.026	24.054	26.217
13	4.107	4.765	5.892	7.042	8.634	12.340	16.985	19.812	22.362	25.472	27.688
14	4.660	5.368	6.571	7.790	9.467	13.339	18.151	21.064	23.685	26.873	29.141
15	5.229	5.985	7.261	8.547	10.307	14.339	19.311	22.307	24.996	28.259	30.578

[1] Table 1 is abridged from Table IV of Fisher and Yates: "Statistical tables for biological, agricultural and medical research," published by Oliver and Boyd Ltd., Edinburgh, and is published by permission of the authors and publishers.

distribution of the 3 sections within each group was random was then tested. There are 9 values in section A, 11 in section B and 10 in section C. According to the hypothesis 9/30 or 30% of the values in each group are expected to be classed as section A, similarly 11/30 or 36.7% as section B and 10/33 or 33.3% as section C. Since there are 6 values in each group the expected number for section A is 1.8, section B 2.2 and section C 2.0. Computations are given below for the test on group II.

$$\text{(unadjusted)} \quad x^2 = \frac{(1 - 1.8)^2}{1.8} + \frac{(4 - 2.2)^2}{2.2} + \frac{(1 - 2.0)^2}{2.0}$$

$$= 0.355 + 1.473 + 0.500$$

$$= 2.328$$

From the Chi-square tables in Table 3 it is seen that 2.328, with 2 degrees of freedom has a probability (Pr) of being random of between 0.50 and 0.20. All computations are summarized in Table 4. For a 5 (group) x 3 (section) block arrangement the number of degrees of freedom are determined by the formula:

d.f. = (no. of Chi-square values) minus (no. of rows plus no. of columns minus one)

$$= (3 \times 5) - (3 + 5 - 1) = 8$$

In this case the Pr of less than 0.01 indicates that the distribution of the 3 sections within the 5 groups is not random and the new hypothesis can again be easily rejected at the 0.05 level of significance. It is notable that the larger the departure of group and section values from the expected distribution, the larger the Chi-square index and the greater the implication of cause and effect.

TABLE 4

SUMMARY OF CHI-SQUARE TEST RESULTS FOR ROUNDNESS (SECTION) VALUES

Group	Number of Values	Observed Section Values			Expected Section Values			Computed Chi-Square (Unadjusted)	Degrees of Freedom	Probability of Randomness
		A	B	C	A	B	C			
I	6	6	0	0	1.8	2.2	2.0	14.000	2	0.01
II	6	1	4	1	1.8	2.2	2.0	2.328	2	0.50 - 0.20
III	6	1	1	4	1.8	2.2	2.0	3.009	2	0.50 - 0.20
IV	6	1	4	1	1.8	2.2	2.0	2.328	2	0.50 - 0.20
V	6	0	2	4	1.8	2.2	2.0	3.818	2	0.20 - 0.10
Sum of Chi-Squares								25.483	8	0.01
Total for Area	30	9	11	10	9	11	10			

The above tests have shown, at a high level of significance, that the size and shape measurements strongly indicate the existence of a non-random pattern, and since the groups have been shown to exist in a non-random pattern these groups (postulated zones) have been established on a quantitative basis.

Figure 3 (fold out) shows the topographic profiles, with zonal limits and sampling points located, below which the first four moment measures of the sediment size distribution at each sample point are plotted separately against distance. The sediment size curves for each sample point are drawn above the topographic profiles. These same topographic profiles appear in Fig. 4, together with separate graphs for percentage fines by weight in the sediment samples and for the mean length, mean roundness, mean sphericity and mean flatness of the constitutent stones, each plotted against distance. Both sets of topographic profiles are exaggerated x5 in the vertical and the zero elevation line represents mean sea level.

Upon cursory examination of Fig. 3 it is apparent that the size distribution of the surface material is a dominant factor in distinguishing zonal types. Size distriburions in phi size units, as obtained from the SEDANL program, have been plotted against weight in grams above each of the sample points. These graphs provide a visual presentation of the unimodal distribution of coarse material in the talus zone which changes downslope to the bimodal distributions of finer material in the solifluction and raised beach zones, which subsequently grade back into the unimodal distributions of the coarser active beach material (Fox, Ladd, and Martin 1966).

Mean phi size graphs plotted immediately below each topographic profile express the pronounced changes of size, associated with those of the size distributions, and are plotted on a vertical scale of 0.0 ϕ to 6.0 ϕ. Moving downslope the average size of surface material on the three profiles decreases rapidly from -5.43 ϕ at the base of the talus to -3.29 ϕ at the lower limit of the upper solifluction zone, primarily as a result of fine material being washed out of the sub-surface talus debris. The size reduction may also be the result of mechanical corrasion within the solifluction zone. An increase in surface water flow in the lower solifluction zone increases the percentage of surface fines and lowers the overall size to -0.44 ϕ. Upper raised beach deposits immediately downslope are on the average larger, reflecting a change in process from mass movement weathering to insitu disintegration. Since the degree of disintegration is largely a function of time in sedimentary rocks the extent of frost-shattering and chemical weathering decreases toward the more youthful active beach, hence material becomes larger (photos 12 - 16). The anomally of a decrease in size from the lower limit of solifluction to the upper limit of the raised beach zone on profile 1 (Fig. 3) can then be explained in terms of the elevation of the material in that area; since the more elevated the marine deposit the longer it has been exposed to insitu weathering. In this case, enough time has passed to allow the reduction of the surface debris to the consistency of coarse sand. Another change of process is indicated, by size, in the active beach zone, where upper zones represent an area built up by ice push action and storm waves, exhibiting the relatively large size of -5.10 ϕ, on the average. Below

this, smaller gravel berms are built representing the normal energy conditions of the beach.

Standard deviation plotted against distance (Fig. 3) provides an index of sorting at each sample point, where the zero reference line denotes perfect sorting. The close relationship between ϕ size and standard deviation suggests that the larger the material the better the sorting. Standard deviations are therefore lowest in the high energy environments of the talus and active beach zones. Decreases in ϕ size and degrees of sorting in the central zones reflect the lower energy regime dictated by more gentle slopes and subdued relief.

Energy conditions are also reflected in the distribution of skewness values plotted against distance (Fig. 3) where the zero line represents a perfectly symmetrical sample distribution. Values range from 0.0 to 1.84 indicating an overall positive skewness or tendency to a tail of fine material to the right of each size distribution. Notably the largest and best sorted distribution in the peripheral high energy areas have the lowest skewness values, except the talus sample 2.9 where a small tail of fines, representing 1.15% of the sample by weight results in a high skewness value. Central low energy areas are characterized by bimodal distributions having much higher skewness values as a function of a marked increase of the percentage of fine material.

Kurtosis, the fourth and most sensitive moment measure is plotted against distance and varies above and below the reference line of +3, the value of a mesokurtic distribution. Kurtosis values more than +3 imply a more peaked than normal or leptokurtic distri-

bution as a result of extremely long tails. In general, changes in skewness and kurtosis values occur in the same direction, the magnitude of change being greater in the fourth moment measure reflecting small differences in the ϕ size distributions. Despite this sensitivity the kurtosis graphs do not allow any differentiation between high and low energy regimes. Assymetry of distributions as found in the high energy environments of the raised beach and talus zones produce platykurtic curves (values less than +3), but the bimodal distributions of the central zones also produce platykurtic curves. It is in the development of long tails of fines to produce leptokurtic or peaked curves that the sensitivity of the fourth moment measure is best expressed. These leptokurtic values occur as abrupt anomalies to the general trend and appear to indicate the points of maximum change in the delicate associations of form and process.

Percentage fines by weight plotted against distance in fig. 4, although a function of time, is strongly controlled by the type and amount of water movement across the topic area. Profile 2 exhibited the greatest amount of fine material on the surface, being the direct result of surface water flow, mainly rill wash, whereas the lower amount of fines on profiles 1 and 3 coincides with much dried conditions.

The second set of graphs in fig. 4, mean length in mm closely reflects phi size and is mainly attributable to the same causes. However, where phi size distribution values are greatly affected by the percentage fines, mean length is a significant modifier of mean roundness, mean sphericity and mean flatness.

Plotted against distance the roundness graphs in fig. 4 display an initial trend of increasing roundness downslope from the very angular

talus material to the lower limit of the solifluction zone. This is accompanied by a decrease in mean length, therefore in light of Cailleux' roundness formula (roundness = $\frac{2R}{A}$ x 1000) it is impossible to establish how much of the increase in mean roundness is due to actual rounding and how much the roundness values are artificially increased by a decrease in length (A). This effect is most marked at the upper limit of the raised beach zone on profile 1, where the change of process to frost shattering should decrease roundness as seen on profiles 2 and 3, but instead the roundness value increases. Downslope roundness values increase, reflecting the marine origin of the material. Roundness values in the active zone decrease progressively going northward from profile 1 to profile 3, thus roundness as a function of depositional energy can be equated to the actual form of the foreland in this zone.

Rock type contributes to decreasing sphericity in the upper zones of the area, since much of the breakdown occurs along the laminar planes of weakness in the sedimentary rocks producing flat plates. As a result there is a very close inverse relationship between sphericity and flatness which would probably not occur in non-sedimentary rock disintegration. The fourth and fifth graphs of mean sphericity and mean flatness show the marked change of process across the solifluction to the raised beach to the active beach zones. But again length (A) serves to artificially vary the magnitude and direction of sphericity and flatness changes particularly on profile 1 but flatness by Cailleux (flatness = $\frac{A + B}{2C}$ x 100) is logically not affected by length as much as sphericity by Krumbein (sphericity = $\sqrt[3]{\frac{B.C}{A^2}}$). The above general

summary of conditions as interpreted from Figures 3 and 4 are refined in the following zone by zone description.

CHAPTER IV

The Talus and Solifluction Zones

Talus slopes in the topic area are generated from an initial free face or cliff, produced by the emergence of an overdeepened valley, which has been subjected to intense frost action. Upland plateau drainage, where concentrated along the free face increased weathering at these points and cones of debris accumulated below these areas. This differential backwasting of the cliff face produced an irregular series of talus cones below gorges developing at the edge of the upland plateau. Overall backwasting continued until the composite talus almost completely buried the free face. Near the top of the talus more resistant beds now protude as ledges and tors (photo 4).

Frost-riving and the supply of water to effect this action are largely coincident with the frequency and magnetude of peripheral plateau gorge development. These gorges become self perpetuating entities since they in turn provide drainage depressions into which more snow will accumulate. The growth of the talus cone progresses until a seasonal stream is formed above it, which then begins to dissect the talus cone itself. In the topic area only one gorge had developed to this extent, the remainder of the talus slope remaining in the stage of aggradation. Fine material in the subsurface appears to increase downslope and can be seen as the direct product of frost

and water action on argillaceous shales and coarse grained crinoidal sandstones. Larger material composing the surface veneer is composed of shattered debris of the more massively bedded limestones and dolomites. Some larger rocks often roll directly from the freeface to the bottom of the talus and beyond littering the immediate downslope areas. But most large rocks disintegrate while bouncing down the talus slope accounting in part for the surface layer of large and extremely angular surface material. In this respect the conical talus forms act to deflect larger material to either side of the cone. Slopes reflect the size of material and vary from 36° in the larger material between the zones to 22° down the axis of the cones, however all slopes approach the general angle of rest of 35° near the top of the cliff.

All slopes are vegetation free due to the high mobility of the surface material. There is also a general uniformity of material source, aspect and time of free face exposure as seen from the similarity of size and shape measurements of samples taken from the base of the talus cones (samples 1.9, 2.9 and 3.9 in Table 1). Roundness values in fig. 4 are extremely low as surface material is not only angular but mean lengths (A) are relatively large. Squaring the length (A) using Krumbein's sphericity formula produces high values since the width (B) and thickness (C) are near the dimensions of length, $\left(\sqrt[3]{\frac{B.C}{A^2}}\right)$, similarly flatness values are low as expected.

The talus zone, although uniform on the surface is the most heterogeneous in composition and constitutes or has constituted most of the source material for the four other zones. Measurements of slope, form, size and shape all point to the perpetually youthful

nature of the surface material. It is a zone characterized by a high degree of potential energy, this energy released in the kinetic form by water and particle novement, the force of gravity and frost-riving being the main triggers.

The Solifluction Zone

A major feature of the instability of surface terrain in periglacial climates has been encompassed under the general heading of solifluction. For the purposes of this study this movement has been termed seasonal creep as defined by Washburn (1867), "a discontinuous process resulting from differential movement of 'soil' particles within the soil mass due to volumetric changes on wetting and drying or freezing and thawing". The amount and nature of the solifluction material strongly suggests its origin as that of the subsurface fines in the talus cones. Aspect, slope, depth of the active layer and the degree of soil moisture largely control this type of mass wasting and lead to a differential accumulation and distribution of surface material. The greatest extension of the solifluction material is mainly dependent upon the area of maximum drainage density from the upland plateau and on the area over which this drainage spreads downslope (photo 3). Thus at the northern end of the topic area drier conditions and more confined avenues of surface water flow restrict the development of the solifluction zone despite steeper slopes.

Immediately downslope from the talus zone the surface area of the foreland is more than 50% covered by solifluction material. Generally upper slopes are hummocky due to relatively high vertical

velocities common to heaving. Further downslope the convex slopes grade to slightly concave as horizontal velocities increase and solifluction terraces, commonly one meter high, begin to form. A sharp reduction in vertical velocity occurs beyond the convex, lobate form and the final solifluction terrace. These slopes are more gentle and surface flow (rillwash) is the major agent of downslope transportation. On the basis of vertical velocities the whole solifluction area has been divided into two zones; the upper solifluction zone, from the lowest solifluction terrace to the base of the talus and the lower solifluction zone constituting the remaining downslope solifluction debris. These will be discussed as separate entities.

Before proceeding with a detailed discussion, the effects of an ancient terrace, three larger streams and a boulder field require some comment. As seen from Fig. 2 and from topographic profiles 1 and 2 there is a large terrace of approximately 400 feet in width and 200 feet in height. This terrace may represent a former beach which was built out then maintained or eroded back to form a well defined beach. This may be evidence of a change in offshore topography associated with either emergence, or evidence of polycylic emergence or a function of change in the rate of emergence or finally a change in the supply of the material to the beach. As a definable unit the terrace becomes more obscure going northward degenerating into an unorganised series of hummocky solifluction lobes negating the possibility of its structural origin. Progressive terrace disintegration provides an additional supply of material for the extended solifluction area in association with varying amounts of ground water.

Three major streams dissecting the topic area provide a good crossection of the type of surface water flow in a periglacial climate. The northernmost stream is the largest, having cut its own gorge which extends downslope to the sea. Of a smaller magitude is the southernmost stream cutting a gorge through the old beach terrace and gradually dissipating in the lower solifluction zone. Smallest of the three, the central stream does not exhibit any extensive gorge development but spreads out immediately below the remnants of the old beach terrace. These streams have a common ephemoral nature characterized by a short period of peak discharge. A general estimate by J. B. Bird (1967) states that as much as 80% of the total annual discharge may occur over as little as 3% of the year. Even diurnal variations can be notable. All three streams in the topic area showed extensive braiding, meandering and steep sides in the loose debris.

Deep gullying has confined the largest stream to a limited area of action significantly reducing the surface water supply to the surrounding solifluction areas enhancing form stability and definition. Gullying, in the upper reaches of the southernmost stream similarly enhances the stability of the old terrace to the south. Farther downslope the second stream fans out spreading fine material by surface rill wash extending the solifluction area far downslope. The central stream, although much smaller is the most effective agent of surface mass wasting producing a marked increase in percentage fines. Towards the lower end of the zone slow moving surface water spreads out to form shallow pools of almost stagnant water at the time of maximum melting. Fine silts are deposited in these pools to an inch or more

in depth, some also settle out in the swales of the downslope raised beach material.

The third anomally, a boulder field,presents an obstacle to the movement of solifluction material on its southern side and tends to stabilize the gorge slopes on the northern side. (Refer to Fig. 2). The angular nature, varied size, lack of sorting, and evidence of abandoned, braided stream channels persists in the boulder field to about 200 feet from the lower end. In this last 200 feet heaving and mass movement can be readily seen beneath the main rubble surface, possibly obscuring former stream channels. The origin of the boulder field may thus be entirely fluvial. Its termination in the upper raised beach material may be explained by isostatic uplift of the general area in conjunction with a northward shift in the position of the stream bed which would leave the boulder field in the apparent erratic circumstance. Other explanations including snow avalanche debris, or debris accumulation at the base of an ancient ice slope may account for the high frequency of very large (greater than 200 cm.), angular boulders found in the lowest 200 feet of the boulder field.

Turning to size and shape, the marked decreases in ϕ are very closely matched by proportionate increases in percentage of surface fines by weight. Zone width of the solifluction area coincides with the increase of fine material, hence surface water flow. Profiles 1, 3 and 2 show a respective increase in zone width as expected from the comments on the three streams previously mentioned. Refer to fig. 3. It was also expected that roundness ($\frac{2R}{A} \times 1000$) and sphericity ($\sqrt[3]{\frac{B.C}{A^2}}$) values would increase as implied by a decrease in ϕ size and length (A),

but this does not occur. From talus to upper solifluction zones roundness increases in all cases (sample 9 to sample 8). The increase of roundness despite an increase in length at top of profile 1 implies an overall increase in absolute roundness below the talus zone. Decreasing values of sphericity associated with increasing flatness are the direct result of rock type, i.e., laminar fracture. Changes downslope to the end of the upper solifluction zone (sample 7) may now be seen more clearly. Downslope increasing roundness on profile 1 is most probably due to a decrease in length, since roundness values decrease on profiles 2 and 3 despite decreases in length. Frost-riving or laminar corrasion fracture must therefore be the agents of reduction of the larger particles in the debris. This is reinforced by a continuing decrease in sphericity values on profiles 2 and 3 associated with an increase in flatness values. But it must be kept in mind that length also acts to artificially raise sphericity values as seen in profile 1 (sample 8 to sample 7).

The above arguments apply to the lower solifluction zone as well (samples 5 and 6). A general decrease in size downslope from the upper solifluction zone is accomplished by an increase in percentage fines and a decrease in mean length. This engenders an increase in roundness, however, on profile 3 the reverse holds true, where size and length increase yet roundness still increases. In all profiles then it is probable that an increase in absolute roundness is taking place. Sphericity is again controlled more by flatness than by length. The more youthful nature of the surface material in the vicinity of profile 3 may be seen to cause decreasing sphericity values produced

by an incomplete breakdown of both angular and laminar talus material. Going southward an increase in age and/or amount of surface water have allowed a greater degree of modification of the original material to produce an increase of sphericity from sample 6 to sample 5.

Over the whole solifluction area a well defined association of patterned ground exists. The upper areas are characterized by heaving, producing sorted and non-sorted circles and nets of small, less than 50 cm. diameter. These grade into unsorted stripes downslope becoming more sorted with additional water as on profile 2. Sorted and non-sorted stripes give way to polygonal patterns in the lower solifluction areas as horizontal and vertical velocities within the surface layer decrease. Along the lower limit of the zone frost cracks from distinct polygonal nets. These nets, although generally of a non-sorted type, are commonly made up of water deposited fines. On a smaller scale the fine material appears to follow a polygonal pattern produced by dessication during the dry cold season and are not destroyed by the slow moving water of the wet season. Larger nets are sorted on the extreme margins of the solifluction area but no frost fissures are developed. Patterned ground across the solifluction zone reveals a progressive increase in the organisation of the surface material going downslope from a higher to a lower energy environment and is closely associated with the amount of surface water, the size distribution and standard deviation of the material. Vegetation reflects this, becoming more dense and widely distributed downslope.

Areas of solifluction are the most extensive and easily definable units of surface modification found on arctic slopes, but

the unit is only a surface entity, of extremely variable composition, form and distribution. Slope, rock type, aspect and water appear to be the dominant controlling factor in the creation and extension of solifluction material. In many cases, but specifically in the topic area this unit extends downslope over raised beach material, the next zone in the foreland sequence.

CHAPTER V

The Raised and Active Beach Zones

Raised beach material constitutes the subsurface debris of the solifluction zone. Downslope surface expression of this material from the lower limit of the solifluction zone to the sea is seen as a series of raised strandlines. Similar to the solifluction zone the beach material may be treated as a total area, then divided into the raised beach zone and the active beach zone for more detailed comments. Age or time of surface exposure has a more marked effect than surface water, in fact, the beach zone is much drier than the solifluction zone, thus a distinct change of process takes place from unstable to stable or insitu weathering. Frost shattering, selective solution and wind winnowing become the predominant agents of the weathering complex (photo 5). This change between zones is not as abrupt as the change between the talus and solifluction zones. There exists instead a discontinuous band of imbricated, or upended rock fragments, the band being of variable width and generally covered with mossy vegetation. Width and generally covered with mossy vegetation. Width appears dependent on horizontal subsurface velocities which persist immediately below the solifluction zone and is therefore controlled by moisture and slope. As a result width of the imbricated area becomes broader going northward as a function of the greater amount of water in the vicinity of profile 2 and the steeper solpes of profile 3, but the

increase in width is accompanied by a decrease in definition. Material is extremely angular as imbrication allows a greater exposure to frost shattering in the limestone fragments and to the force of corrasive fracture by subsurface movement (photo 6).

Beyond the imbrication band the difference between the solifluction and the beach material becomes more distinct as strandline relief progressively increases downslope reaching a maximum on the active beach. Surface material to a depth of approximately 10 cms contains variable amounts of fines, time of exposure controlling the extent to which material is broken down. Sample 4 at the top of the raised beach zone therefore exhibits a higher percentage of fine material than the relatively younger exposures downslope. Concentration of these fines in the swales of the strandline system may be accounted for by the accumulation of water in these areas promoting frost shattering. Secondly fine material tends to be transported to the swales, by both water and wind, from the strandline ridges. Generally, the drier the surface, the more pronounced the removal of ridge fines by wind winnowing. Downslope material contains progressively fewer fines evidencing a decrease in the extent of insitu weathering until almost no fines are present in the active beach material.

Vegetation decreases perceptably downslope until the surface, on the active beach zone, is completely devoid of growth. Swales as areas of moisture accumulation allow some of the most dense and luxurious growth of vegetation in the topic area but these vegetation patches exist as anomalies to the general downslope decrease in growth. Patterned ground likewise decreases downslope. Some sorted nets occur

in the swales of the raised beach zone, however, the most common pattern is produced by the frost fissure. It is striking that these fissures are arranged in a trellis rather than a polygonal pattern, no doubt attributable to the linear nature of the raised strandline relief.

Turning to changes of size and shape, it was expected that insitu weathering would produce a larger, more angular fragment than did solifluction activity, sample 5 to sample 4. Upon investigation, however, this was seen to be only partly true. Profile 1 of fig. 3 shows a decrease in size below the solifluction zone instead of the expected increase. Here the extensive width of the raised beach zone implies a long time of exposure allowing a great deal of disintegration to have taken place at the top of the zone. Lack of surface water has curtailed the extension of the solifluction debris downslope on profile 1, but on profile 2 the creep debris has moved much farther downslope, therefore, the raised beach material at the top of the zone is relatively much younger resulting in a distinct increase in size at sample 4. Profile 3 is in an intermediate condition where drier condition have been overcome somewhat by steeper slopes to allow more overriding of the raised beach material by solifluction than on profile 1, but less than on profile 2. It should also be kept in mind that the elevation of the raised beach strands are closer to sea level on profile 3 and the increase in ϕ size reflects this youthful condition.

Referring to fig. 4, the first graph of percentage fives inversely follows the above argument in the raised beach zone. Length, a close direct association with ϕ size, decreases sharply on profile 1 at sample 4, producing an artificially high roundness value. A decrease

in flatness ($\frac{A + B}{2C}$ x 100) follows the decrease in length (A), which in turn increases sphericity. Profiles 2 and 3 show the opposite effect where more youthful surface material retains more of its original marine character. Marked increases in length engender decreases in roundness and flatness, the later reducing sphericity values.

It was expected that roundness, sphericity and size would increase going downslope on the raised beach zone from sample 4 to sample 3. This occurs on all profiles except profile 1, where roundness and sphericity values decrease as size increases. Yet surface material, from direct observation becomes noticeably rounder and more spheroidal going downslope. In this case roundness and sphericity as well as flatness are changing purely due to a change in size and length and not in absolute terms. Shape values on profiles 2 and 3 are, however, valid indicators of what is observed and expected despite conflicting changes in size and length. This dichotomy will be discussed in the next chapter.

Changes again are distinct between the active and raised beach zones. An unstable increase in relief is visible on the profiles of Figures 3 and 4. Another difference is one of colour. Dull brown-yellow of varying hues, dependent on moisture, is characteristic of the raised beach zone but the active beach zone is a uniform light grey. On profile 1 this change occurs gradually over a distance of approximately 100 feet but on profile 3, where slopes are steeper and the zones narrower this change of colour occurs in less than 10 feet.

Upper ridges of the active beach are "storm" ridges produced by large magnitude, low frequency wave and ice action. Lower ridges

are of a more ephemoral nature owing their formation to diurnal and seasonal changes in sea and ice conditions. The active beach zone is further disrupted by the presence of ice push debris and ice mounds. The former are the product of the ramming of ice flows up the beach during freeze-up. These flows melt in the spring to leave a levelled path lined with striations culminating in a small mound of bulldozed debris often in a crescentic shape. In some cases these push mounds maintain their form into the raised beach zone, but more probably large flows extend over the active and into the raised beach zone (photos 7 and 8). Ice mounds on the other hand are near shore features. Their formation has been attributed to shore ice buckling, ice flow stacking and to the accumulation of marginal ice built up in conjunction with tidal action. The last of these explanations seems most probable in light of the large amount of interstitial debris within the ice mound. The mound shape is a product of differential ablation of the debris-laden ice. As melting occurs an accumulation of debris on the top insulates the ice beneath. Further melting occurs as this debris slides off the mound, but the melting is slow enough to allow the ice mound to remain longer after snow and ice have been dissipated. These mounds are undercut by waves during open sea conditions and finally topple into the sea. Aside from a small mound of debris deposited on the beach they leave little effect on overall relief and form of the beach. However, both the ice mound debris and the ice push debris serve to contribute to a poor organisation of active beach material (photos 9, 10 and 11).

This lack of uniformity can be seen from the changes in size and length, samples 1 and 2 on figures 3 and 4, thus roundness and sphericity values appear to be random. Two points of uniformity are worth comment. There is a conspicuous lack of fines and there is no surface modification, secondly the upper limits of the zone are generally of a larger ϕ size due to the higher energy of ice and wave action required to build these ridges.

The active beach zone is one of maximum and most frequent change, yet in width it is the most uniform of all zones. This relatively narrow, high energy environment is the most youthful aspect of the depositional foreland - the most variable in organisation and form but the most stable in genisis and continuity.

CHAPTER VI

Regression Analysis

Associated changes of size and shape measurements require further quantitative analysis, principally to evaluate the measurements themselves. Seven of these interrelated variables, frequently referred to in preceding chapters, have been subjected to a multiple regression analysis to establish the type and degree of correlation between them. Standard deviation, skewness and kurtosis values of ϕ size distributions have been omitted since moment measure correlations were not considered pertinent to the correlations. Percentages of free carbonates were also omitted, due to incomplete sampling.

Size in phi units, the most consistent indicator of change, was chosen as the dependent variable. Mean roundness, mean flatness, mean sphericity, mean length in m.m., percentage fines by weight, and slope in degrees were chosen as the six most diagnostic parameters to relate or "explain" the variations in mean ϕ size for computation in the multiple regression program written by D. R. Ingram. An overall linear correlation coefficient of 0.95105 was obtained indicating that 90.5% of the variation in ϕ size units was accounted for by changes in the six independent variables (Krumbein 1965).

Referring to the attached computer output, individual correlation coefficients illustrate the relative strengths of these variables. The laminar nature of sedimentary rock fragments become less pronounced as

CORRELATION COEFFICIENTS

ROW 1								
1.00000	0.02142	-0.09166	-0.20816	0.09595	-0.70581	-	0.40568	roundness 4
ROW 2								
0.02142	1.00000	-0.94010	0.41839	-0.11782	-0.31134	+	-0.26138	flatness 6
ROW 3								
-0.09166	-0.94010	1.00000	-0.43457	0.20370	0.32000	-	0.32166	sphericity 5
ROW 4								
-0.20816	0.41839	-0.43457	1.00000	-0.66264	0.27193	+	-0.82814	length 1
ROW 5								
0.09595	-0.11782	0.20370	-0.66264	1.00000	-0.24332	-	0.80401	% fines 2
ROW 6								
-0.70581	-0.31134	0.32000	0.27193	-0.24332	1.00000	+	-0.51079	slope 3
ROW 7								
0.40568	-0.26138	0.32166	-0.82814	0.80401	-0.51079		1.00000	ϕ size
roundness	flatness	sphericity	length	% fines	slope		ϕ size	

- very high negative correlation between flatness and sphericity (-0.94010)

All ϕ size units greater than 1 m.m. are prefaced by a negative index correlation signs must be multiplied by (-1)

\+ length
\- % fines
\+ slope
\- roundness
\+ sphericity
\- flatness

in decreasing degree of correlation with ϕ size

1.0 added to % fines values

SELECTION... 1

VARIABLE NO.	MEAN	STANDARD DEVIATION	CORRELATION X VS Y	REGRESSION COEFFICIENT	STD. ERROR OF REG. COEFF.	COMPUTED T VALUE
1	137.38889	64.17859	0.40568	0.00216	0.00192	1.12953
2	399.25926	110.03673	-0.26138	0.00156	0.00236	0.66183
3	0.56185	0.05193	0.32166	6.98265	4.87453	1.43248
4	36.83333	8.58442	-0.82814	-0.04944	0.01522	-3.24730
5	11.98148	15.55346	0.80401	0.03274	0.00735	4.45738
6	9.62963	7.88937	-0.51079	-0.04045	0.01766	-2.29019
DEPENDENT						
7	-3.96926	1.16298				
INTERCEPT		-6.99620				

MULTIPLE CORRELATION	0.95105
STD. ERROR OF ESTIMATE	0.40978

- 90.5% of variation in ϕ size explained by changes in the 6 dependent variables

ANALYSIS OF VARIANCE FOR THE REGRESSION

SOURCE OF VARIATION	DEGREES OF FREEDOM	SUM OF SQUARES	MEAN SQUARES	F VALUE
ATTRIBUTABLE TO REGRESSION	6	31.80739	5.30123	31.57005
DEVIATION FROM REGRESSION	20	3.35839	0.16792	
TOTAL	26	35.16578		

physical and chemical disintegration progresses, the textural properties becoming more evident. This is especially true of the shales and crinoidal sandstones, these two lithologies accounting for a significant proportion of the finer material. These changes measured by length in mm. closely match changes over the same area in ϕ size units to the degree of +0.82814. As mentioned previously, the amount of surface water and the time over which disintegrating processes have been active is associated with the percentage of surface fines. The weight of these fines in grams is also highly correlated with size in phi units (-0.80401) but inversely, as seen from figures 3 and 4. Samples of these fines taken from profiles 1 and 2 were tested in the laboratory to determine their percentage composition of free carbonate by weight using the Collins Calcimeter method. Values ranged from 61.0% to 23.0% and appeared to decrease systematically downslope from a maximum at the solifluction terraces of the upper solifluction zone. Although these values were not used in the multiple correlation computations it is expected that the values of free carbonates by weight would not correlate highly with ϕ size units since the former values decrease continually in a downslope direction. The third most highly correlated variable, slope in degrees relates to ϕ size units to the magnitude of +0.51099. Here the values of slope are in many cases closely related to the size of the material on them.

Shape measurements of roundness and flatness by Cailleux and sphericity by Krumbein have attempted to integrate the above conditions and variables into a composite form. To an extent they have both succeeded as seen from the tests carried out on roundness and sphericity values to establish the existence of non-random areal distributions over

the topic area. But they have some distinct disadvantages. Roundness values, calculated according to the formula $\frac{2R}{A} \times 1000$, where A is the length and R the radius of least curvature in the plane of the A axis, are modified to a great extent by the length A. The regression correlation of roundness with size is therefore low (-0.40568) and only 16.5% of the changes in size can be related to changes of roundness. The formula incorrectly assumes that a change in size is mutally inclusive with an increase in the radius of curvature, when in many situations the opposite is true, especially in the case of frost shattering. A further disadvantage of this method is in the measurement of R, by matching the radius of least curvature to concentric millimeter circles on a chart. The subjectivity of this measurement was evident when a test for operator bias was carried out on a sample of 50 pebbles. Computed mean roundness values varied up to 11%, despite a difference in mean lengths (A) of less than 1%.

Flatness values on the other hand are more accurate and repeatable since only discrete measurements are used in Cailleux' formula $\frac{A + B}{2C} \times 100$, where A, B and C represent length, width thickness respectively. Despite a low correlation coefficient (+0.26138) with size, flatness values are twice as closely associated to length as roundness values, rock structure being the controlling factor. Structure is therefore significant in determining sphericity in light of the very high negative correlation (-0.94010) of sphericity with flatness. Sphericity holds the same advantage of accuracy and repeatability using Krumbein's formula, $\sqrt[3]{\frac{B.C}{A^2}}$, however, the effect of squaring the length (A) promotes a further dissociation from ϕ size.

Measured in equal units, ϕ size is converted from a linear metric scale to a logarthmic one according to Wentworth's formula, $\phi = \log_2 d$, where d is the particle diameter in millimeters. A comparison of phi size to sphericity can then have no more meaning than a comparison of an assymptole to an hyperhola, as illustrated by the low correlation coefficient (-0.32166) of sphericity with ϕ size units. Krumbein's formula may be more meaningfully expressed as $\sqrt[3]{\frac{\log_2 B \cdot \log_2 C}{2 \log_2 A}}$ where changes in A, B and C would vary on the same scale as ϕ size. The above formula will not be evaluated in this study but it is hoped it will prove valid in putting shape measurements into a more workable frame of reference. It is this lack of reference which is the most restricting aspect of shape measurements, without it changes of magnitude of shape cannot be significantly compared or evaluated in terms of the discrete measures of ϕ size, length, percentage fines and slope.

CHAPTER VII

Conclusions

By way of summary the distributions of mean roundness, mean sphericity and mean particle size were all shown to have a probability of non-randomness of greater than 95% over the topic area as a whole and within each zone. On a more detailed scale each zone has been proven to change according to a general trend associated with explainable anomalies. Finally a multiple regression analysis permitted a succinct evaluation of the measurements employed, revealing particle size to the most relevant and consistent parameter of change. Thus size distributions and shape characteristics of the samples taken from the surface mantle of the Cape Ricketts foreland have been shown to be conducive to the illustration of a distinct morphogenetic system - a system changing definably and predictably downslope and alongslope. These changes are so marked that the extensive dimensions of the sample grid and the limited number of pebbles in each sample measured for shape (20) did not detract significantly from the accuracy of the data.

The zonal hypothesis was then tested, by observation, on the northern slopes of Beechy Island 7 miles to the west of Cape Ricketts. Certain differences affecting the sequential development of zones were apparent on Beechy Island, notably rock type and structure. The sedimentary structure was more massive than in the Cape Ricketts area, sandstones of a finer grain and lower crinoidal composition. Disintegration appeared to take place much more quickly, producing a high

percentage of fines over the whole surface area. Secondly relief of the cliff top was some 150 to 200 feet lower than at Cape Ricketts, the talus material in some cases obscuring the free face completely. In general, though, talus slopes were much less extensive as would be expected from their northerly exposure. Chemical weathering of great intensity was indicated by deeply solution pitted plates of frost shattered limestones as well as massive scales of secondary calcite precipitation on the underside of most pebbles in the raised beach zone.

Thirdly, the solifluction zone has developed much more extensively and erratically, covering a greater relative downslope area of the raised beach material than on the Cape Ricketts foreland. Slopes were generally steeper, surface rill wash almost entirely lacking, and overall percentage fines higher, as a consequence of which the upper solifluction zone is greatly extended whereas the lower solifluction is only developed to a limited extent. Differences in the active zone are less marked, being attributable to the presence of shore ice and lack of wave action dictated by changing annual ice conditions.

Although the continuity of the zones across slope was not consistent at Beechy Island the 5 segments did exist as recognisable, sequential surface forms. The zonal hypothesis was considered valid, at least from a qualitative point of view as no samples were collected.

On the coastal slopes of southern Cornwallis Island, near Resolute Bay, however, no definable sequence of zones were found. Immediate onshore relief is generally too low to generate extensive

talus slopes, but more significantly the sedimentary rocks are dipping at an angle greater than 10 degrees to the southwest. Nearly horizontal bedding must then be considered as one of the prerequistes for sequential zone development. Cape Ricketts presents a somewhat ideal case of a definable morphogenetic system common to the emergent landform of plateau, cliff and raised marine deposits of the Eastern Arctic.

1. Coastline of S.W. Devon Island looking west. Plateau, cliff and raised marine material constitute the majority of landforms. Vertical Cliffs on the eastern exposure of Beechy Island in the middle ground are 600 feet high.

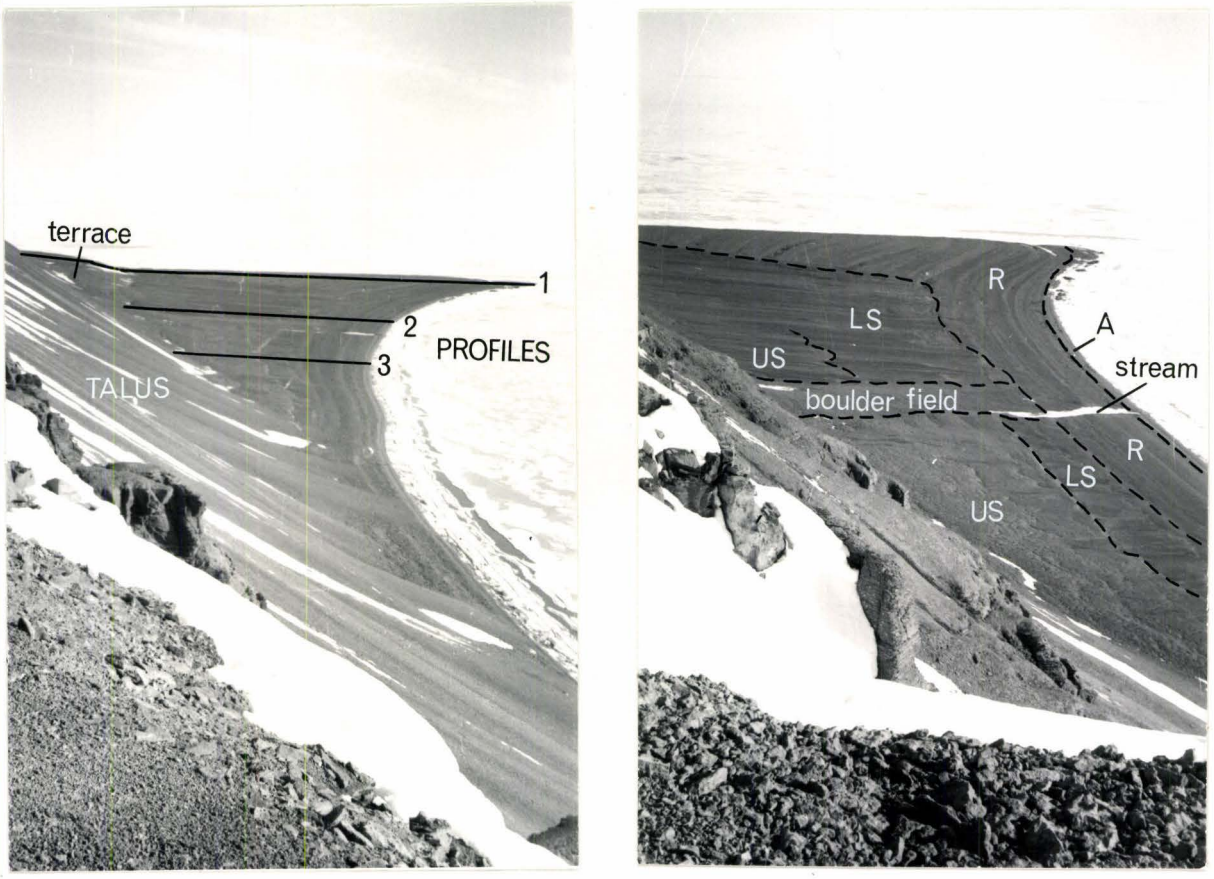

2. Two views of the Cape Ricketts foreland, looking due south from the edge of the upland plateau. The photograph to the left illustrates the general narrowing of zones going north until completely overridden by talus material. Zones stand out clearly in the righthand photograph, solifluction terraces being quite distinct in the foreground. Beyond the main stream gorge and boulder field, surface water flow significantly modifies solifluction activity. Continuity of raised strandlines is also notable.

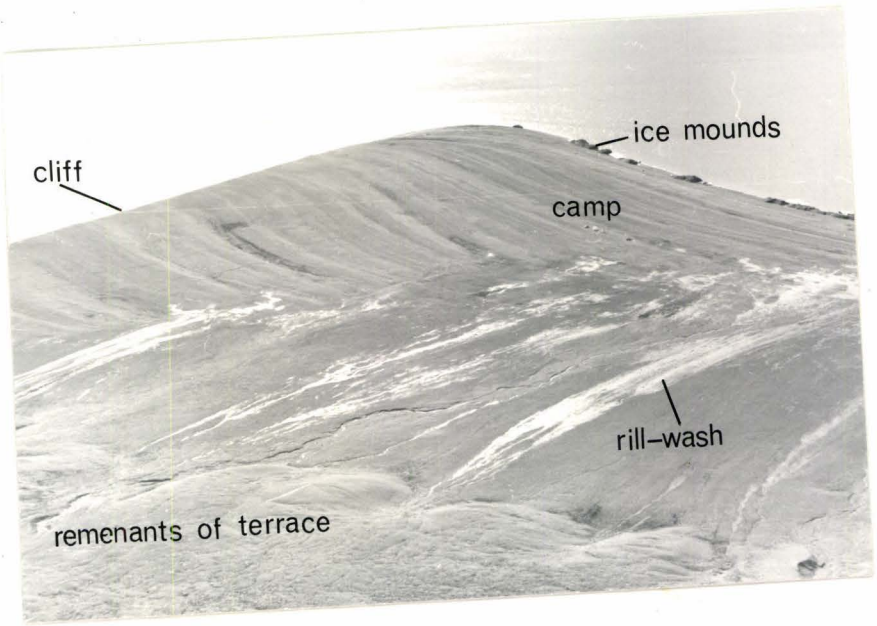

3. View of the southern end of the Cape Ricketts foreland showing the effects of water as an agent of surface modification.

4. View of the northern end of the Cape Ricketts beach. Note the large, angular talus debris littering the raised beach zone and the change of colour and relief in the active beach zone.

5. The depth and degree to which insitu chemical and physical weathering has progressed in modifying raised beach material in the vicinity of profile 1 approximately 100 feet above sea level

6. Platy, partially imbricated, limestone fragments resulting from frost-shattering surround the debris circle of a completely disintegrated crinoidal sandstone boulder.

7. Striations in the foreground have been produced by ice flows rammed up the beach, terminating in the debris mounds in the background

8. A close up view of the ice push debris mounds in the raised beach zone.

9. Ice mound covered with ablation debris is approximately 16 feet high.

10. The effect of wave action is to undercut the mound which at first maintains a cantilever form, the base frozen to the permafrost.

11. Wave action eventually cuts away the base of the ice mound, which topples into the sea leaving a small mound of debris similar to ice push material.

Representative samples of material measured for shape from profile 2.

13. Smaller but still quite angular material of the final solifluction terrace - 50.1% fines not shown.

15. Much rounder and larger material of the lower raised beach zone - no fines.

12. Large, angular talus material - no fines.

14. Rounder pebbles from the transition zone between solifluction and raised beach material - 32.4% fine not shown.

16. Active beach material, showing distinct rounding - no fines.

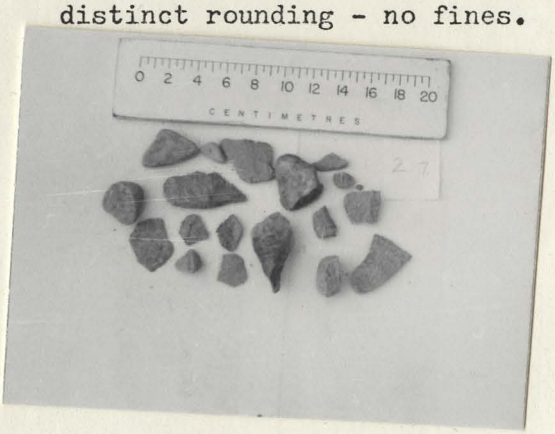

FIG. 3

GRAPHS OF THE TOPOGRAPHIC PROFILE AND THE FIRST FOUR MOMENT MEASURES PLOTTED AGAINST DISTANCE

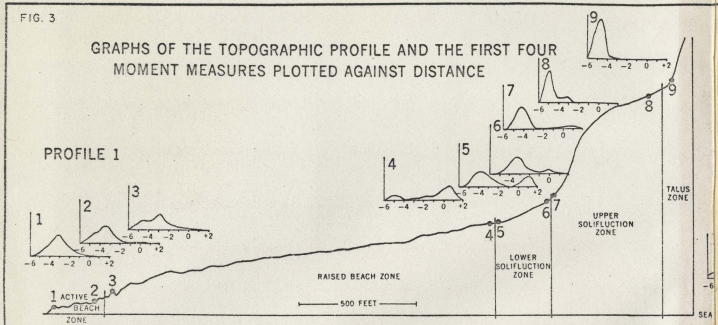

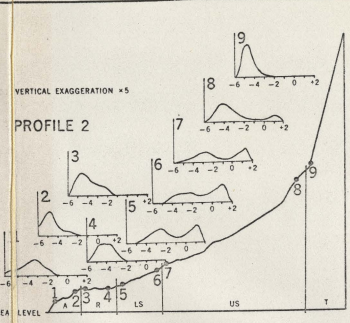

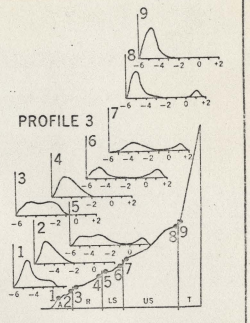

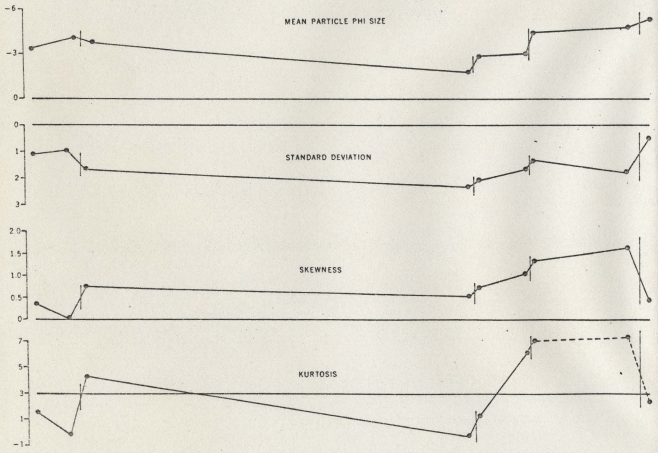

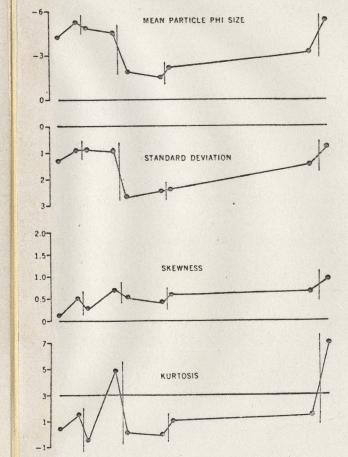

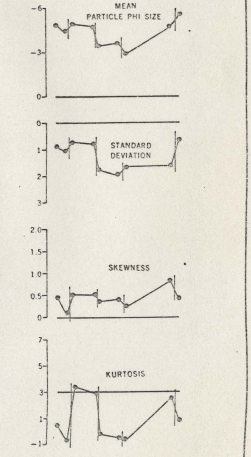

FIG. 4

GRAPHS OF THE TOPOGRAPHIC PROFILE, PERCENTAGE FINES, AND FOUR MEASURES OF SHAPE PLOTTED AGAINST DISTANCE

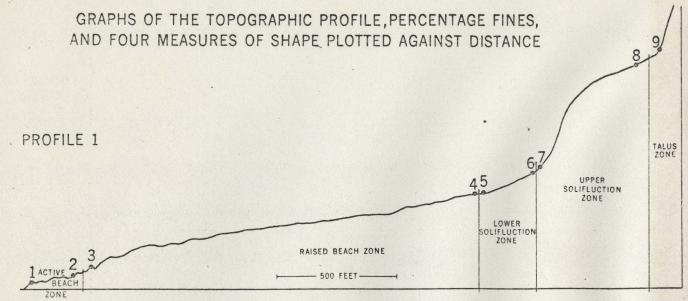

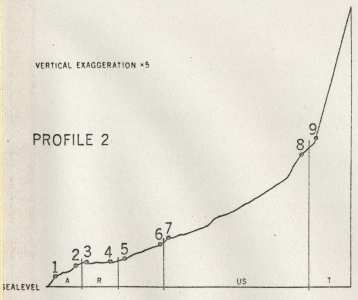

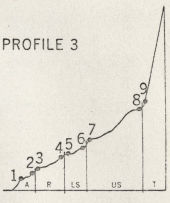

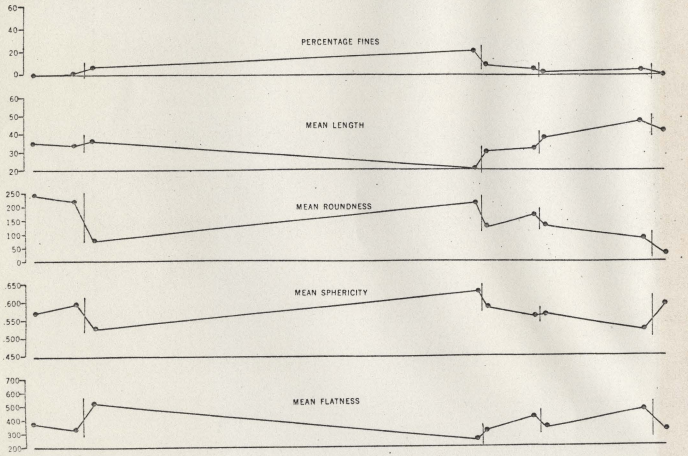

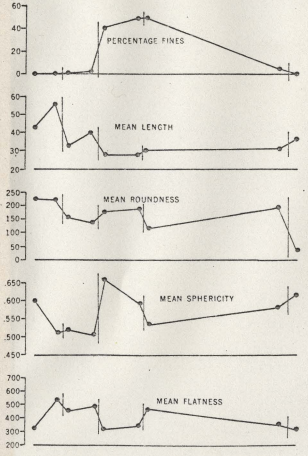

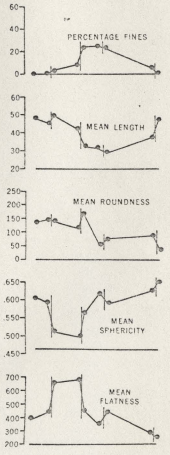

REFERENCES

Bird, B.J., 1967, The Physiography of Arctic Canada, pp. 257-271

Cadigan, R.A., 1962, A method for determining the randomness of regionally distributed quantitative geologic data. Journ. Sed. Petrol., vol. 32 no. 4, pp. 813-818.

Cailleux, A., 1945, Distinctions des galets marines et fluviatiles. Bull. Soc. Géol. France, 5 s, 15, pp. 375-404.

Cailleux, A., and Tricart, J., 1963 and 1965, Initiation à l'étude des sables et des galets. 1 - Texte, 1963: 2 - Valeurs Numeriques, Morphoscopie des sables, 1965: 3 - Valeurs Numeriques, galets granulometrie, Morphometric et nature des sables, 1965. Centre de Documentation Universitaire, Paris.

Fox, W.T., Ladd, J.W., Martin, M.K., 1966, A profile of four moment measures perpendicular to a shoreline, South Haven, Michigan. Journ. Sed. Petrol., pp. 1126-1130.

Inman, D.L., 1952, Measures for describing the size distributions of sediments, Journ. Sed. Petrol., vol. 22, pp. 125-145.

King, C.A.M., and Buckley, J.T., 1968, The analysis of stone size and shape in the Arctic environment. Journ. Sed. Petrol., 3.8(1) pp. 200-214.

Krumbein, W.C. and Graybill, F.A., 1965. An Introduction to Statistical Models in Geology. McGraw-Hill, New York, pp. 221-248.

Krumbein, W.C. and Pettijohn, F.T., 1938, Manual of Sedimentary Petrology.

------, 1952, The sorting out of geological variables by regression analysis of factors controlling beach firmness. Journ. Sed. Petrol., 29, pp. 575-587

Mason, C.C., and Folk, R.L., 1958, Differentiation of beach dune and aeolian flat environments by size analysis, Mustang Island, Texas. Journ. Sed. Petrol., 28, pp. 211-226.

Schlee, J., and Webster, J., 1965, A computer program for grain size data. Technical Report 65-42, Woods Hole Oceanographic Institute, Massachusetts. Unpublished manuscript.